

# EVALUATION OF EMPC FOR ATTITUDE CONTROL OF AAUSAT3

Anders Bech Borchersen

*Department of Electronic Systems  
Aalborg University, December 2010  
Group 930, 10gr930@es.aau.dk*

**Abstract**—This paper studies whether explicit model predictive control is suited to use for the attitude control for a CubeSat satellite using magnetic actuation. As a case the student satellite AAUSAT3 is used. The EMPC is compared with two classical controllers designed for AAUSAT3. From the results found through simulations, it is concluded that EMPC might not be suited for the use of attitude control of AAUSAT3 instead a classical controller should be used.

**Index Terms**—Explicit Model Predictive Control, AAUSAT3, Attitude Control, Magnetic Actuation, CubeSat

## I. INTRODUCTION

The purpose of this paper is to explore suitable algorithms for the Attitude Control System for CubeSat sized satellites like AAUSAT3.

AAUSAT3 is the third student satellite developed at Aalborg University. The Attitude Determination and Control System (ADCS) is essential for the AAUSAT3 mission [1] during operation. The ADCS system can be in one of the three general states shown in Fig. 1. A detumble controller which ensures

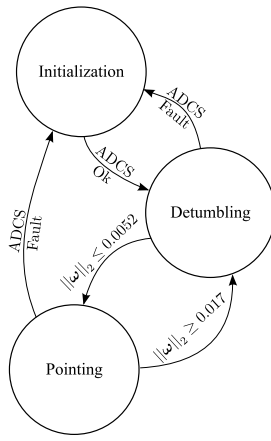


Fig. 1. The three general states for the ADCS system on AAUSAT3

stability has been design and tested [2] for the detumbling state. An Attitude Determination System (ADS) has been designed and tested [2] which is necessary for the pointing state, for which two different Attitude Control Systems (ACS) has been designed and tested. These are a constant gain controller [3] and a Non-linear Model Predictive Control(NMPC) [2]. The ACS using the constant gain controller is feasible for AAUSAT3 but it requires approximately 2 orbits before settled and when settled the performance is not impressive.

The controller based NMPC performed satisfying but showed to be infeasible, since it required the solving of a non-convex optimization problem online, and do to the limited computation power available on AAUSAT3 the use of NMPC is not feasible for AAUSAT3.

Thus it is investigated if Explicit Model Predictive Control (EMPC) can be used for the ACS on AAUSAT3. Since it has been shown that it can be used to control a CubeSat sized satellite, where the actuation system consisted of magnetic actuators as the active actuation and a gravity boom for passive actuation [4].

Furthermore EMPC have been used for attitude control of non-CubeSat sized satellite where thrusters and momentum wheels are the available actuators [5]. In both case the performance of the EMPC was satisfying.

On AAUSAT3 the only available actuation is magnetic actuation thus the hypothesis tested in this paper is: *Can Explicit Model Predictive Control be used for attitude control of a CubeSat sized satellite like AAUSAT3?*

In this paper a short introduction to EMPC is given in Section II-A, then the model of the satellite is briefly described and linearized in Section II-B. Then four different controllers suited for AAUSAT3 are designed in Section III, two based on EMPC and two based on the LQR. Then these controllers are tested in the simulation environment in Section IV, then in Section V a discussion evaluating on the achieved results, based on the discussion it is concluded which controller to use for the attitude control on AAUSAT3 in Section VI.

## II. METHOD

The following description for a discrete-time linear state space system is used

$$\mathbf{x}_{t+1} = \mathbf{Ax}_t + \mathbf{Bu}_t \quad (1)$$

$$\mathbf{y}_t = \mathbf{Cx}_t + \mathbf{Du}_t \quad (2)$$

Where  $\mathbf{x}_t$  is the state.  $\mathbf{A}$  the system matrix.  $\mathbf{B}$  the input matrix.  $\mathbf{u}_t$  the input.  $\mathbf{y}_t$  the output.  $\mathbf{C}$  the output matrix.  $\mathbf{D}$  the feed-forward matrix and is assumed to be 0 thus omitted from here and on. It is assumed that the pair( $\mathbf{A}, \mathbf{B}$ ) is stabilizable.

### A. Explicit Model Predictive Control

The basic idea of EMPC is to calculate a explicit solution to the model predictive controller (MPC). This is done by first converting the linear MPC problem to a Quadratic Programming (QP) problem which then is reformulate to

a multi-parametric quadratic programming(mp-QP) problem. When using MPC the following convex optimization problem is solved for each time step

$$\min_{\mathbf{U}} \quad J(\mathbf{U}, \mathbf{x}(t)) = \mathbf{x}_{t+N_y|t}^T \mathbf{P} \mathbf{x}_{t+N_y|t} + \sum_{k=0}^{N_y-1} \mathbf{x}_{t+k|t}^T \mathbf{Q} \mathbf{x}_{t+k|t} + \mathbf{u}_{t+k}^T \mathbf{R} \mathbf{u}_{t+k} \quad (3)$$

$$\text{s.t. } \mathbf{u}_{\min} \leq \mathbf{u}_{t+k} \leq \mathbf{u}_{\max}, k = 0, \dots, N_u - 1 \quad (4)$$

$$\mathbf{y}_{\min} \leq \mathbf{y}_{t+k|t} \leq \mathbf{y}_{\max}, k = 1, \dots, N_y \quad (5)$$

$$\mathbf{x}_{t|t} = \mathbf{x}(t) \quad (6)$$

$$\mathbf{x}_{t+k+1|t} = \mathbf{A} \mathbf{x}_{t+k|t} + \mathbf{B} \mathbf{u}_{t+k}, k \geq 0 \quad (7)$$

$$\mathbf{y}_{t+k|t} = \mathbf{C} \mathbf{x}_{t+k|t}, k \geq 0 \quad (8)$$

where  $J(\mathbf{U}, \mathbf{x}(t))$  is the cost function there is minimized through the series of inputs  $\mathbf{U} = [\mathbf{u}(k), \dots, \mathbf{u}(k + N_u - 1)]$ ,  $N_y$  is the prediction horizon,  $N_u$  is the input horizon.  $\mathbf{P}$  is the terminal state penalty and might be chosen such that it solves the discrete Lyapunov equation  $\mathbf{P} = \mathbf{A} \mathbf{P} \mathbf{A}^H + \mathbf{Q}$ , if  $\mathbf{A}$  is stable, since if  $\mathbf{P}$  is selected as the solution to the Lyapunov equation then:  $\mathbf{u}_{t+k} = 0$  for  $k \geq N_u$ .

Another solution is to chose  $\mathbf{P}$  such that it is a solution to the discrete algebraic Riccati equation  $\mathbf{P} = \mathbf{A} \mathbf{P} \mathbf{A} - (\mathbf{A}^T \mathbf{P} \mathbf{B})(\mathbf{R} + \mathbf{B} \mathbf{P} \mathbf{B})^{-1}(\mathbf{B} \mathbf{P} \mathbf{A}) + \mathbf{Q}$ . This will lead to a LQR controller for  $k \geq N_u$  [6], and this might be preferred for unstable  $\mathbf{A}$ .

$\mathbf{U}^*$  is the sequence of inputs that minimized (3). Subject to the constraints in (4) to (8). To find  $\mathbf{U}^*$  the prediction problem stated in (3) can be reformulate to QP problem [7]:

$$\frac{1}{2} \mathbf{x}^T \mathbf{Y} \mathbf{x} + \min_{\mathbf{U}} \frac{1}{2} \mathbf{U}^T \mathbf{H} \mathbf{U} + \mathbf{x}^T \mathbf{F} \mathbf{U} \quad (9)$$

$$\text{s.t. } \mathbf{G} \mathbf{U} \leq \mathbf{W} + \mathbf{E} \mathbf{x}. \quad (10)$$

The solution for the QP problem is convex if  $\mathbf{H} > 0$ . To solve the QP problem good solvers are available [8], thus a solution can be found. But still the QP problem has to be solved for every time step. To avoid the online computation required to solve the QP problem, an explicit solution for the QP problem can be found [9]. This is done by converting the quadratic program in (9) to a multi-parametric quadratic program(mp-QP) problem. By defining

$$\mathbf{z} \equiv \mathbf{U} + \mathbf{H}^{-1} \mathbf{F}^T \mathbf{x} \quad (11)$$

which then transforms the QP problem from (9) into the mp-QP problem [10]

$$\min_{\mathbf{z}} \frac{1}{2} \mathbf{z}^T \mathbf{H} \mathbf{z} \quad (12)$$

$$\text{s.t. } \mathbf{G} \mathbf{z} \leq \mathbf{W} + (\mathbf{E} + \mathbf{G} \mathbf{H}^{-1} \mathbf{F}^T) \mathbf{x} \quad (13)$$

A solution to the mp-QP problem can be found [10] [11] and is a PWA function pending on the state  $\mathbf{z}$  which is then a variable of the system state  $\mathbf{x}$ . Thereby the online computation is reduced to find the region corresponding to the current state, and then calculate and apply the control signal [12].

To find a solution to the mp-QP problem the Multi-Parametric Toolbox (MPT) [13] is used in Matlab. The description and solving of the EMPC is done by following these steps [14]:

- 1) Scale the matrices and states/inputs so they are well scaled (exploit  $\pm 10$ )
- 2) Have as few dynamics as possible when designing a PWA system model.
- 3) Have as few states and inputs in the system model as possible.
- 4) Use the largest possible sampling time when discretizing the system.

### B. Modelling

In this section the model of the satellite is derived. The following notation for the frames are used:

$^i$  denotes the earth centered initial reference frame (ECI)

$^c$  denotes the controller reference frame (CRF)

$^o$  denotes the Orbit Reference Frame (ORF) where the Z axes is pointing towards the center of the earth the X axes is in the direction of the orbit plane.

The rotation matrix between ORF and CRF is defined as  ${}^c C_o$ .

To describe the kinematics of the satellite the attitude of the satellite is described by quaternions, to avoid singularities when representing the attitude, the following notations for the quaternions is used:

$$q_1 = e_1 \sin\left(\frac{\theta}{2}\right) \quad q_2 = e_2 \sin\left(\frac{\theta}{2}\right) \quad (14)$$

$$q_3 = e_3 \sin\left(\frac{\theta}{2}\right) \quad q_4 = \cos\left(\frac{\theta}{2}\right) \quad (15)$$

$$\mathbf{q} = [q_1 \quad q_2 \quad q_3 \quad q_4]^T \quad (16)$$

$$1 = \sqrt{q_1^2 + q_2^2 + q_3^2 + q_4^2} \quad (17)$$

where  $e_1, e_2, e_3$  describe the eigenaxis and  $\theta$  is the rotations about the eigenaxis.

The kinematics is given as [15]:

$$\dot{\mathbf{q}} = \frac{1}{2} \begin{bmatrix} \mathbf{S}(\boldsymbol{\omega}) & \boldsymbol{\omega} \\ -\boldsymbol{\omega}^T & 0 \end{bmatrix} \mathbf{q} \quad (18)$$

The dynamics for the satellite is derived by first deriving the model for the inertial to the CRF and then expanded to the ORF. The change in angular momentum is given as [15]:

$$\dot{\mathbf{L}} = \sum_{i=1}^n \mathbf{N}_i \equiv \mathbf{N} \quad (19)$$

where  $\mathbf{L}$  is the angular momentum vector and  $\mathbf{N}$  is the torque from external forces (disturbances- and control-torques). The angular momentum in CRF is:

$${}^c \mathbf{L} = {}^c \mathbf{C}_i^i \mathbf{L} \quad (20)$$

$$(21)$$

When derived it can be rewritten to

$${}^c \dot{\mathbf{L}} = -{}^c \boldsymbol{\omega}_{ci} \times {}^c \mathbf{L} + {}^c \mathbf{N} \quad (22)$$

using the following relations

$${}^c \dot{\mathbf{C}}_i = -{}^c \boldsymbol{\omega}_{ci} \times {}^c \mathbf{C}_i \quad (23)$$

$${}^c \mathbf{N} = {}^c \mathbf{C}_i^i \dot{\mathbf{L}} = {}^c \mathbf{L} \quad (24)$$

The angular momentum of a rigid body is given as

$$\mathbf{L} = \mathbf{I}\boldsymbol{\omega} \quad (25)$$

Where  $\mathbf{I}$  is the inertia matrix. The angular momentum in the CRF can there by be written as:

$${}^c\mathbf{L} = \mathbf{I}^c\boldsymbol{\omega} \quad (26)$$

$${}^c\dot{\mathbf{L}} = \mathbf{I}^c\dot{\boldsymbol{\omega}} \quad (27)$$

By substituting (27) into (22) the following representation of  ${}^c\dot{\boldsymbol{\omega}}_{ci}$  is obtained:

$${}^c\dot{\boldsymbol{\omega}}_{ci} = \mathbf{I}^{-1} (-{}^c\boldsymbol{\omega}_{ci} \times \mathbf{I}^c\boldsymbol{\omega}_{ci} + {}^c\mathbf{N}) \quad (28)$$

It is desirable to have the satellite pointing towards nadir. Therefore the model is written such that it describes the relation with respect to the ORF and CRF instead of the ECI and CRF as above. This is done by using the following relationship between the angular velocities of the frames:

$${}^c\boldsymbol{\omega}_{ci} = {}^c\boldsymbol{\omega}_{co} + {}^c\mathbf{C}_o^o\boldsymbol{\omega}_{oi} \quad (29)$$

$${}^c\dot{\boldsymbol{\omega}}_{ci} = {}^c\dot{\boldsymbol{\omega}}_{co} + {}^c\dot{\mathbf{C}}_o^o\boldsymbol{\omega}_{oi} \quad (30)$$

It is assumed that the speed between ORF and ECI is constant about the y axes since the orbit is approximately circular and thereby  ${}^o\boldsymbol{\omega}_{oi} = [0 \ \omega_0 \ 0]$ . The non-linear model for the satellite is can then be written as:

$$\begin{aligned} {}^c\dot{\boldsymbol{\omega}}_{co} &= \mathbf{I}^{-1} \left( -({}^c\boldsymbol{\omega}_{co} + {}^c\mathbf{C}_o^o\boldsymbol{\omega}_{oi}) \times \mathbf{I}({}^c\boldsymbol{\omega}_{co} + {}^c\mathbf{C}_o^o\boldsymbol{\omega}_{oi}) \right) \\ &\quad + \mathbf{I}^{-1} {}^c\mathbf{N} + {}^c\boldsymbol{\omega}_{co} \times {}^c\mathbf{C}_o^o\boldsymbol{\omega}_{oi} \end{aligned} \quad (31)$$

To design a linear regulator as the EMPC a linear model of the satellite is required, thus the non-linear model in (18) and (31) is linearized. To have a linear model on the form of (1), the following state vector is used  $\mathbf{x} = \begin{bmatrix} \mathbf{q} \\ {}^c\boldsymbol{\omega}_{co} \end{bmatrix}$ . To point towards nadir the linearization is done around:  $\bar{\mathbf{x}} = [0 \ 0 \ 0 \ 1 \ 0 \ 0]^T$ . Then by first order Taylor approximation derived in [3] the  $\mathbf{A}$  is given as

$$\mathbf{A} = \begin{bmatrix} 0 & 0 & 0 & 0.5 & 0 & 0 \\ 0 & 0 & 0 & 0 & 0.5 & 0 \\ 0 & 0 & 0 & 0 & 0 & 0.5 \\ -2k_x\omega_0^2 & 0 & 0 & 0 & 0 & (k_x + 1)w_0 \\ 0 & 0 & 0 & 0 & 0 & 0 \\ 0 & 0 & 2k_z\omega_0^2 & (k_z - 1)w_0 & 0 & 0 \end{bmatrix} \quad (32)$$

Where  $k_x = \frac{i_{yy}-i_{zz}}{i_{xx}}$ ,  $k_y = \frac{i_{zz}-i_{xx}}{i_{yy}}$ ,  $k_z = \frac{i_{xx}-i_{yy}}{i_{zz}}$ . For the linear model the following should be noted: q4 is removed from the system model since it is given by the other quaternions and is uncontrollable. This leads to the following state vector  $\tilde{\mathbf{x}} = \begin{bmatrix} \mathbf{q}_{1:3} \\ {}^c\boldsymbol{\omega}_{co} \end{bmatrix}$  for the linearized system. It should be noted that torque generated from the gravity is seen as a disturbances, and thus not include in the linear model since it so small for a CubeSat with almost equally principle moments of inertia.

### C. Magnetic Actuation

The actuation available on AAUSAT3 is magnetorques. These actuate by generating a local magnetic field which then gives a torque perpendicularly to Earths magnetic field. This leads to a time varying  $\mathbf{B}$  since the actuation can not be performed when the generated magnetic field is parallel to Earths magnetic field.

Furthermore the strength and direction of the Earth magnetic field varies over a single orbit and is also changing over several orbits this can be seen in Fig. 2. Where the direction and the strength of the magnetic field in the three axes is plotted over 30 orbits seen from the ORF. The variations in

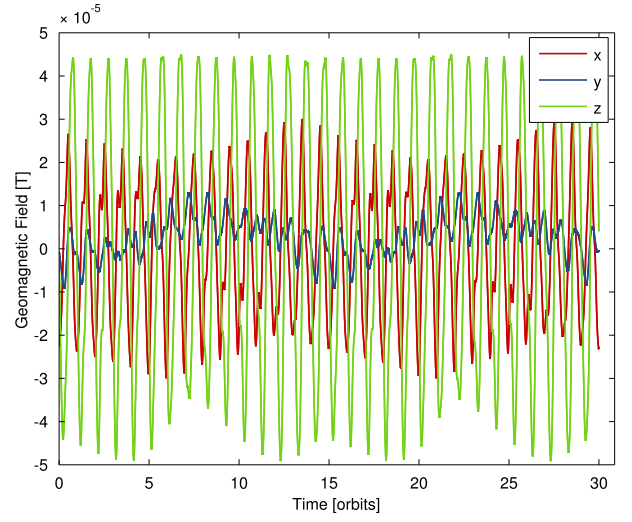


Fig. 2. Plot of the geomagnetic field in the ORF over 30 orbits

the magnetic field leads to a non-linear  $\mathbf{B}$  when actuation is done by magnetorques.

To design a linear regulator as EMPC a linear model of the system is required. Thus two approaches to the linearization of the magnetic field is taken.

The first linearization of  $\mathbf{B}$  is found by first approximating the magnetic field to be periodic. Then for each sample time the  $\mathbf{B}_{mag}$  in (33) is calculated and the average of these are found which leads to a constant  $\mathbf{B}_{mag}$  [16].

$$\mathbf{B}_{mag} = \begin{bmatrix} 0 & 0 & 0 \\ 0 & 0 & 0 \\ 0 & 0 & 0 \\ \mathbf{I}^{-1} \begin{bmatrix} -B_y^2 - B_z^2 & B_x B_y & B_x B_z \\ B_x B_y & -B_x^2 - B_z^2 & B_y B_z \\ B_x B_z & B_y B_z & -B_x^2 - B_y^2 \end{bmatrix} \end{bmatrix} \quad (33)$$

The second approach taken to linearization of  $\mathbf{B}$  in the magnetic field is done by dividing the magnetic field into regions. And then use a different  $\mathbf{B}$  for each region. The regions are selected as the octants which are defined by the different sign combination possible for three dimensional space. Since there is no established nomenclature for the octants [17], thus the following numbering of the octants are

used:

$$\begin{Bmatrix} 1(++) & 2(+-) & 3(-+) & 4(--) \\ 5(-++) & 6(-+-) & 7(--+) & 8(----) \end{Bmatrix} \quad (34)$$

For each of the octants the average strength is found and then eight  $\mathbf{B}_{mag1}$  to  $\mathbf{B}_{mag8}$  is derived using the same form as in (33). To verify that the sign of the magnetic field is not changing to often the sign changing of the magnetic field is plotted in Fig. 3.

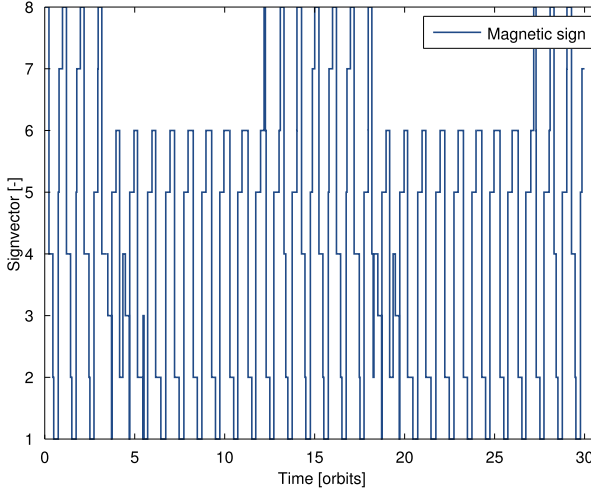


Fig. 3. Plot showing which of the octant the geomagnetic field vector is in seen over 30 orbits from the ORF.

#### D. Full Actuation

Before testing a new controller on a satellite where only magnetic actuation is available. It might be desirable to first verify that the controller can control the satellite when full actuation and no limits on the actuation is assumed. Since this is not physical possible to have such an actuator it is also used to give a upper bound for how good the performance can be. When full actuation is assumed the following  $\mathbf{B}$  is used:

$$\mathbf{B}_{full} = \begin{bmatrix} \mathbf{0} \\ \mathbf{I}^{-1} \end{bmatrix} \quad (35)$$

### III. CONTROLLER DESIGN

In this article four different attitude controllers are compared these are:

- **EMPC Full Actuation** is a controller where full actuation is assumed.
- **EMPC Magnetic Actuation** is an explicit model predictive controller designed for AAUSAT3.
- **Constant Gain Controller** is the classical attitude controller designed for AAUSAT3.
- **Multiple Constant Gain Controller** is a controller consisting of eight constant gain controllers.

The EMPC Full Actuation, EMPC Magnetic Actuation, and Multiple Constant Gain Controller(MCGC) are designed in this paper. The Constant Gain Controller(CGC) was designed

in [3]. There are no requirements specified for the ADCS for AAUSAT3, but it is still desirable to have the pointing towards the nadir, since this increase the performance of the radio link, thus the requirements for the controllers is just to achieve the best possible pointing accuracy. For the angular velocity it is not desirable if  $\|\omega\|_2$  exceeds 0.017[rad/sec], since this will change the state for the ADCS from pointing to detumbling, as shown in Fig. 1.

#### A. Explicit Model Predictive Control with Full Actuation

To design a EMPC a discrete version of the system is required. Thus when discretization is done the sampling time is set to 0.5[sec].

The EMPC where full actuation is assumed, is designed from the linearized system (32) and whit the actuator (35). The design parameters are listed in Table I. The values for  $\mathbf{Q}$  and  $\mathbf{R}$  are found through empirically test. The scaling matrices where found such that the constraints where in the range of  $\pm 10$  the scaling of the system is done by defining the following system:

$$\dot{\mathbf{x}}_{scale} = \mathbf{N}_x^{-1} \mathbf{A} \mathbf{x}_{scale} + \mathbf{N}_x^{-1} \mathbf{B} \mathbf{u}_{scale} \quad (36)$$

where  $\mathbf{x}_{scale} \equiv \mathbf{N}_x^{-1} \mathbf{x}$  and  $\mathbf{u}_{scale} \equiv \mathbf{N}_u^{-1} \mathbf{u}$ . The EMPC controller is then designed for the scaled system. So when implementing it is important to scale the input and output for the controller such that the controller is operating on the scaled system.

When a EMPC is designed from the parameters in Table I using the MPT toolbox. The resulting controller consist of 27 regions. Where for each region the optimal gain matrix and gain are given. It should be noted that when the step horizon is increased the number of regions remains the same(tested for  $N \leq 30$ ). This might indicate that a horizon of 2 is a long enough horizon, for the controller to be able to control the system within the desired state space.

TABLE I  
PARAMETERS USED WHEN DESIGNING THE EMPC WHERE FULL ACTUATION IS ASSUMED

|                       |   |
|-----------------------|---|
| $\mathbf{N}_u$        | diag([1 1 1])   |
| $\mathbf{N}_x$        | diag([1 1 1 10 <sup>-3</sup> 10 <sup>-3</sup> 10 <sup>-3</sup> ])   |
| $\mathbf{Q}$          | diag([0.1 0.1 0.1 300 300 300])   |
| $\mathbf{R}$          | diag([1 1 1])   |
| $N$                   | 2 step (horizon)  |
| Parameter constraints | $-\begin{bmatrix} 1 & 1 & 1 & 10 & 10 & 10 \end{bmatrix} \leq \mathbf{x} \leq \begin{bmatrix} 1 & 1 & 1 & 10 & 10 & 10 \end{bmatrix}$ |
| Actuator constraints  | $-\begin{bmatrix} 1 & 1 & 1 \end{bmatrix} \leq \mathbf{u} \leq \begin{bmatrix} 1 & 1 & 1 \end{bmatrix}$                               |

#### B. Explicit Model Predictive Control with Magnetic Actuation

The EMPC controller with magnetic actuation is designed using the linear system in (32) and  $\mathbf{B}$  from (33). The design parameters used are listed in Table II. The scaling  $\mathbf{N}_u$  and  $\mathbf{N}_x$  where necessary for the MPT toolbox to find a stabilizing controller without giving numerical problems when solving the problem. Then when scaling is applied it changes the constraints of both  $\mathbf{x}$  and  $\mathbf{u}$ . It was observed that the designed controller could not control the satellite do to the weak control

signals, to compensate for this the rescaling of  $\mathbf{u}$  was not performed before the input was applied to the actuator. This might suggest that the actuator available is insufficient for the selected design parameters.

TABLE II  
PARAMETERS FOR THE EMPC CONTROLLER WITH MAGNETIC ACTUATION

|                       |  |
|-----------------------|--|
| $\mathbf{N}_u$        | diag([1 1 1] $10^5$ )  |
| $\mathbf{N}_x$        | diag([1 1 1 $10^{-3}$ $10^{-3}$ $10^{-3}$ ])                                       |
| $\mathbf{Q}$          | diag([6 6 6 300 300 300])  |
| $\mathbf{R}$          | diag([10 10 10])   |
| $N$                   | 2 step (horizon)   |
| Parameter constraints | $-[1 \ 1 \ 1 \ 10 \ 10 \ 10] \leq \mathbf{x}$<br>$\leq [1 \ 1 \ 1 \ 10 \ 10 \ 10]$ |
| Actuator constraints  | $-[0.04 \ 0.04 \ 0.04] \leq \mathbf{u}$<br>$\leq [0.04 \ 0.04 \ 0.04]$             |

### C. Constant Gain Controller

The constant gain controller was designed in [3], thus only an overview is given. Based on the assumption of a constant magnetic field a Linear Quadratic Regulator (LQR) is designed and stability check is done by using the periodic linear system. The LQR parameters are listed in Table III

TABLE III  
PARAMETERS FOR THE CONSTANT GAIN CONTROLLER

|                |   |
|----------------|---|
| $\mathbf{Q}$   | $\begin{bmatrix} \mathbf{Q}_L & \mathbf{Q}_R \end{bmatrix}$ |
| $\mathbf{Q}_L$ | diag[128 128 128]   |
| $\mathbf{Q}_R$ | diag[1.28 1.28 1.28]  |
| $\mathbf{R}$   | diag[1.28 1.28 1.28]  |

### D. Multiple Constant Gain Controllers

The assumption about the magnetic field being constant over time which leads to a constant  $\mathbf{B}$  might be a very rough assumption. A better assumption might be that the magnetic field is constant for each of the octants (34) for the magnetic field as suggested in Section II-C. The eight different input matrices  $\mathbf{B}_{mag1} - \mathbf{B}_{mag8}$  are used for the design of eight constant gain controllers, these are then scheduled according to the sign of the magnetic field. The design parameters for each of the eight controllers is set to the same as for the design of the single constant gain controller, listed in Table III.

## IV. SIMULATION

To verify that the controllers designed is performing satisfying, they are tested using the simulation environment for AAUSAT3. The simulation environment is implemented in Matlab/Simulink and the following disturbances are included in the model Gravity gradient torque, Solar radiation torque, Aerodynamic drag torque, and Magnetic residual torque. For details about the simulation environment see [2]. The controllers are tested in two different tests, to test the controllers in different situations.

### A. The First Test

The first test is performed to verify that the controllers designed in Section III are capable of controlling the satellite. This is done by setting the following start condition for the simulation: The angle between ORF and CRF is set to  $150[\text{deg}]$  and the angular velocity is set to  $0[\text{rad/sec}]$ .

To compare the performance of the two constant gain controllers the rotation between ORF and CRF is compared in Fig. 4, and the velocities are plotted in Fig. 5.

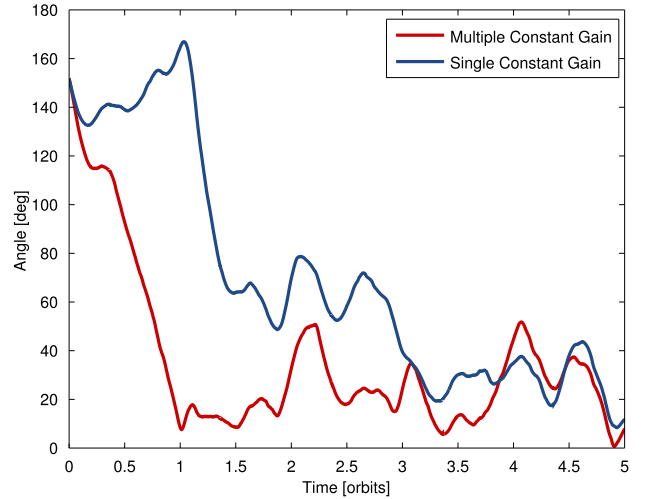


Fig. 4. The eigenaxis angle between ORF and CRF for the Constant Gain Controller(CGC) and the Multiple Constant Gain Controller(MCGC).

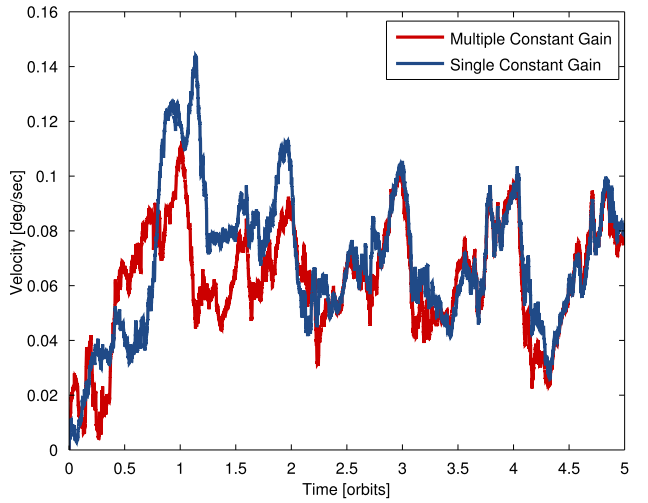


Fig. 5. The norm of the velocity vector for the Constant Gain Controller(CGC) and the Multiple Constant Gain Controller(MCGC).

The angle between ORF and CRF when using the EMPC with full actuation and EMPC with magnetic actuation, are shown in Fig. 6. The norm of the angular velocity for the two EMPC controllers are shown in Fig. 7.

The velocity is significant higher for the EMPC with magnetic actuation than any of the other controllers, the

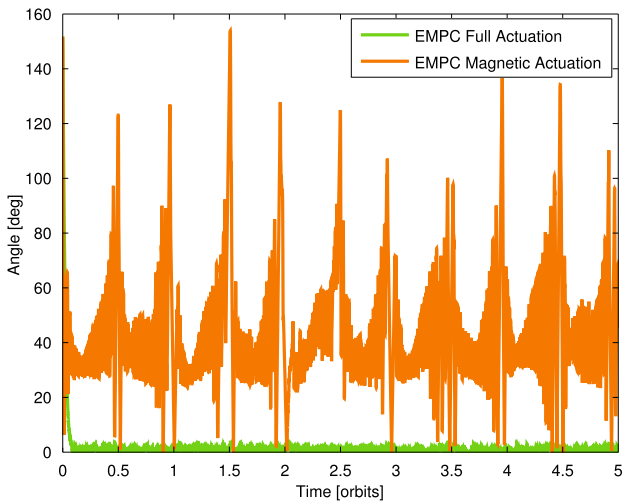


Fig. 6. The eigenaxis angle between ORF and CRF for the EMPC with full actuation.

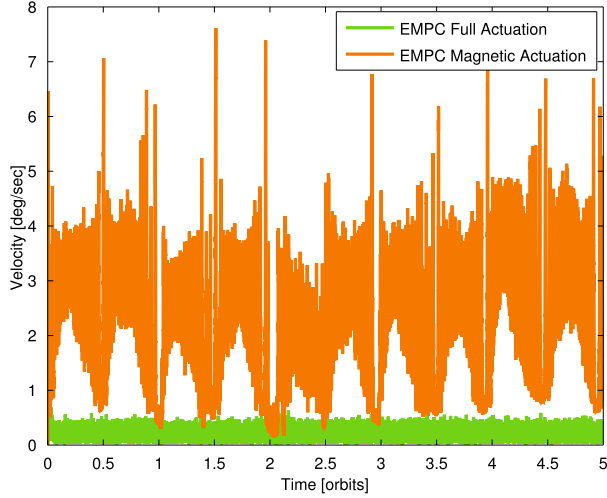


Fig. 7. The norm of the velocity  $c\omega_{co}$  for the two controllers using EMPC.

performance of the EMPC with magnetic actuation is not very impressive when compared to the other controllers. The poor performance might be caused by the EMPC not being able of actuating as expected all the time. A plot of the angle and the strength of the magnetic field is shown in Fig. 8, the plot is showing that when the strength of the magnetic is low the EMPC is not able of keeping the desired angle.

To compare the controllers they are all plotted together in Fig. 9.

#### B. The Second Test

This test should verify if the controller can be used for attitude control on AAUSAT3. To verify this the simulation is now started with an error on the angle and a angular velocity. Since when the satellite is released into space it is expected to have an angular velocity of no more  $0.1[\text{rad/sec}]$  [18]. The high angular velocity will then be reduced to a maximum

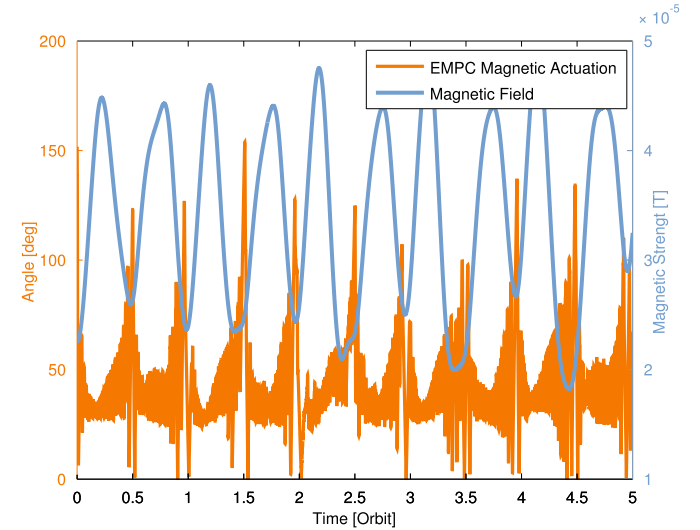


Fig. 8. The EMPC using magnetic actuation plotted together with the strength of the magnetic field.

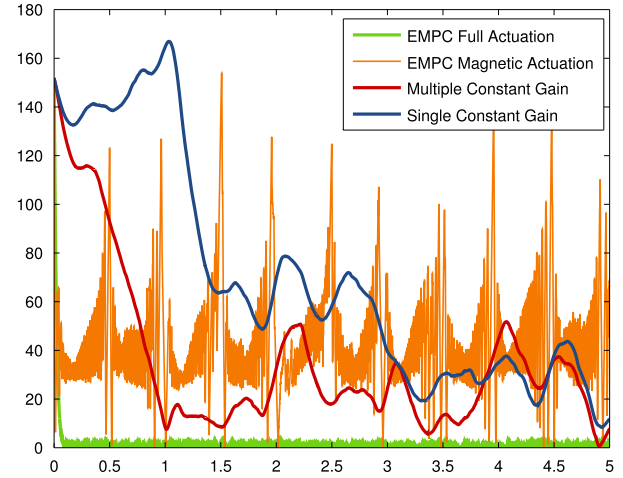


Fig. 9. The angle between ORF and CRF for all four controllers.

of  $\pm 0.0040[\text{rad/sec}]$  by the detumble controller running the B-dot algorithm. Thus for a pointing controller to perform satisfying it should be able to bring the satellite into pointing from an angular velocity of  $\pm 0.0040[\text{rad/sec}]$ . In this test the angle between ORF and CRF is set to  $150[\text{deg}]$  and the angular velocity is set to  $0.004[\text{rad/sec}]$  in all three directions.

This test is only preformed on the MCGC and CGC since these performed satisfying in the first test conducted in Section IV-A. The angle between ORF and CRF for MCGC and CGC is shown in Fig. 10 the 2-norm of the angular velocity vector  $c\omega_{co}$  is shown in Fig. 11

## V. DISCUSSION

In this section the performance of each controller is evaluated based on the results shown in Section IV.

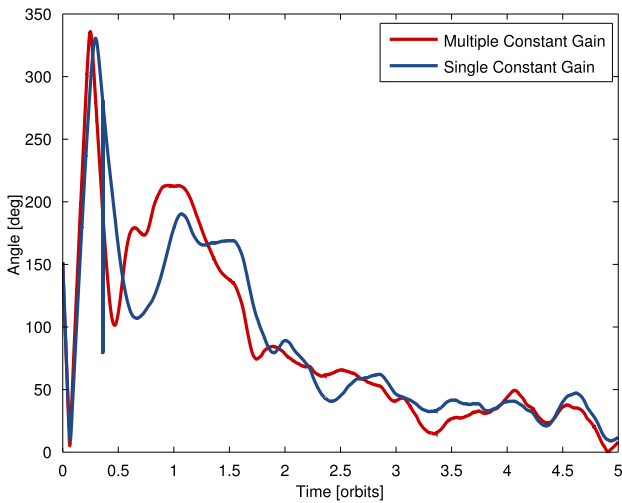


Fig. 10. The angle between ORF and CRF for MCGC and CGC.

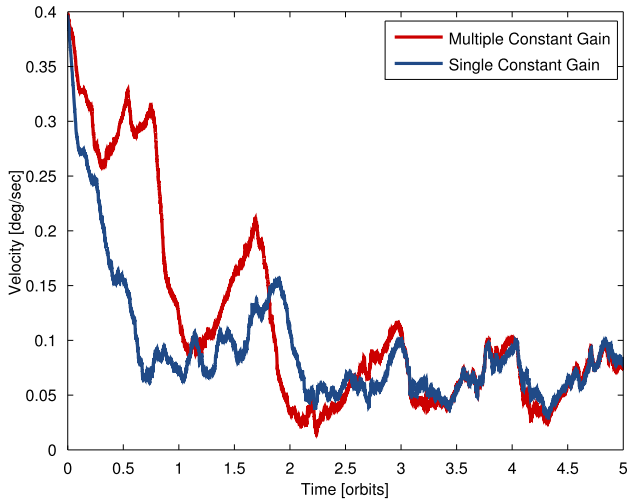


Fig. 11. The norm of the angular velocity vector  ${}^c\omega_{co}$ .

#### A. EMPC Full

From Fig. 9 it is seen that both of the EMPC controllers are very aggressive compared to the CGC and MCGC. As expected the EMPC controller with full actuation is out performing all the other controllers on the pointing accuracy. But to keep this accuracy the controller is having a high angular velocity as seen in Fig. 7. The reason for the high angular velocity might be that the controller is trying to compensate for the disturbances and thus actuation instantaneously when an error on the angle occurs. To avoid the high angular velocities adjusting the  $\mathbf{R}$  and  $\mathbf{Q}$  were tried but without any success.

#### B. EMPC Magnetic

From the results of the EMPC controller having full actuation it is expected for the EMPC controller with magnetic actuation, to perform in the same manner but with reduced performance. This is also the case when the controller is

started and until 0.3 orbits. Then the EMPC with magnetic actuation starts to lose control of the satellite. The reason for this was found due to the variation in the magnetic field. This is seen in Fig. 8 when the strength of the magnetic field is low the EMPC loses control.

The designed EMPC controller consisted of 27 regions, but when the controller was tested it always stayed in the same region. The reason for this might be that since the EMPC is based on the same linear model as the CGC which only requires one single gain matrix to control the satellite. The EMPC algorithm concluded that a single region is enough to control the satellite for most of the constrained state space, and then the last 26 controllers, are only active when the satellite is in the outer regions of the state space and since this never happens no region change occurs.

Different EMPC controllers were tested to get the controller to change regions when controlling the satellite. But these controllers were unstable when tested on the nonlinear model. Furthermore, the number of regions seems to increase to more than 200 and in some cases up to 18000 regions.

Since EMPC is designed using the same linear model as the MCGC is designed from it is questionable if the EMPC can be better than MCGC. Instead of using EMPC on the linear model, better performance might be achieved by using a PWA system description to model the satellite. And thereby give the EMPC more information than the LQR design. To give such a PWA description of the model it would be necessary to increase the number of internal states to define the change of system from an internal state. Thus states describing the changes in the magnetic field would be of great interest to include in the model, thereby the EMPC could adapt to the changing magnetic field which was shown to be the biggest problem for the EMPC.

It should be noted that when using EMPC the number of regions and the description of these greatly increase when the number of states is increased and thereby the online complexity of the controller [12]. Thus the online requirements also increase. So to find a PWA model of the satellite would be interesting if EMPC shall be used for attitude control of a CubeSat size satellite. A way to model the satellite as PWA system might be to assume that the magnetic field only changes between 4 of the 8 octants. Since it can be observed that the magnetic field are in the following four octants most of the time 1, 2, 5 and 6. Furthermore, the order of the change between these octants seems to be the same pattern, this can be seen in Fig. 3, especially from orbit 6 to orbit 13 and again from orbit 20 to 28.

#### C. Constant Gain Controller

The results of the two constant gain controllers from the first test are shown in Fig. 4, where it is seen that the performance of the MCGC was significantly better compared to the CGC. The MCGC used less than one orbit to get the satellite within 50[deg] of the desired angle, compared to the CGC which used three orbits. The angular velocities were approximately the same for the two controllers as shown in Fig. 5. After 3 orbits the two controllers performed equally. So based on

the first test MCGC is faster than CGC to achieve the same performance. This was also expected since the MCGC is scheduled depending on the sign of the magnetic and thereby knows which way to actuate compared to the CGC which requires longer time since it assume a constant magnetic field over time.

In the second test where the satellite had a angular velocity when the simulation was started, the two controllers performed almost identically as seen in Fig. 10 and Fig. 11. Actually the CGC had a lower angular velocity than the MCGC. A reason for the MCGC not performing better than the CGC, might be that when the satellite is having a relative high angular velocity, the magnetic field is changing sign more often, and thus the switching frequency between the different controllers is increase, which might decrease the performance of the MCGC.

## VI. CONCLUSION

Based on the results achieved it is concluded that Explicit Model Predictive Control might not be suited for the attitude control of AAUSAT3, using the current linear model of the satellite. Thus it is either MCGC or CGC to used for attitude control of AAUSAT3. To draw a final conclusion about which one of the two to use a Monte Carlo test might be a way to see which of the two controllers there are the best suited. But based on the tests conducted in this article, the MCGC should be selected for the ACS on AAUSAT3.

## REFERENCES

- [1] “Mission objective for aausat3,” The AAUSAT3 team, 2010, <http://www.aausat3.space.aau.dk/pmwiki.php?n=Site.AISPayload>.
- [2] K. F. Jensen and K. Vinther, “Attitude determination and control system for aausat3,” 2010.
- [3] A. B. Borchersen, B. Eskildsen, K. W. Foged, and J. Lauridsen, “Attitude control and fault detection for aausat3,” 2010.
- [4] T. Krogstad, J. Gravdahl, and P. Tøndel, “Explicit model predictive control of a satellite with magnetic torquers,” in *Intelligent Control, 2005. Proceedings of the 2005 IEEE International Symposium on, Mediterranean Conference on Control and Automation*. IEEE, 2006, pp. 491–496.
- [5] O. Hegrenas, J. Gravdahl, and P. Tøndel, “Attitude control by means of explicit model predictive control, via multi-parametric quadratic programming,” in *American Control Conference, 2005. Proceedings of the 2005*. IEEE, 2005, pp. 901–906.
- [6] D. Chmielewski and V. Manousiouthakis, “On constrained infinite-time linear quadratic optimal control\* 1,” *Systems & Control Letters*, vol. 29, no. 3, pp. 121–129, 1996.
- [7] J. Maciejowski, *Predictive Control with Constraints*. Prentice Hall, ISBN 0-201-39823-0,2002.
- [8] C. OPTIMIZATION, “Using the CPLEX® Callable Library.”
- [9] A. Alessio and A. Bemporad, “A survey on explicit model predictive control,” *Nonlinear Model Predictive Control*, pp. 345–369, 2009.
- [10] A. Bemporad, M. Morari, V. Dua, and E. N. Pistkopoulos, “The explicit linear quadratic regulator for constrained systems,” *automatica*, vol. 38, pp. 3–20, 2002.
- [11] P. Tøndel, *Constrained Optimal Control via Multiparametric Quadratic Programming*. Faculty of Information Technology, Mathematics and Electrical Engineering, Department of Engineering Cybernetics, NTNU, ISBN 8247156083, 2003.
- [12] M. Kvasnica, *Real-Time Model Predictive Control via Multi-Parametric Programming Theory and Tools*. VDM Verlag Dr. M. uller, ISBN 078-3-639-20644-9,2009.
- [13] M. Kvasnica, P. Grieder, and M. Baotić, “Multi-Parametric Toolbox (MPT),” 2004, <http://control.ee.ethz.ch/~mpt/>.
- [14] M. Kvasnica, P. Grieder, M. Baotić, and F. Christoffersen, “Multi-Parametric Toolbox (MPT) Manual,” 2006, <http://control.ee.ethz.ch/~mpt/downloads/MPTmanual.pdf>.
- [15] J. Wertz, *Spacecraft attitude determination and control*. Kluwer Academic Publishers, 1978.
- [16] R. Wiśniewski, *Satellite Attitude Control Using Only Electromagnetic Actuation*. AAU Centertrykkeriet, 1996.
- [17] “Cartesian coordinate system,” Wikipedia, 2010, [http://en.wikipedia.org/wiki/Cartesian\\_coordinate\\_system](http://en.wikipedia.org/wiki/Cartesian_coordinate_system).
- [18] M. Green, M. N. Kragelund, and M. Sletten, “Robust disturbance rejecting attitude control for the north observer satellite,” Aalborg University, Institute of Electronic Systems, 2006.